

Magnetomechanical behavior of a directly solidified Fe-Al-B alloy

Mateus B. S. Dias¹, Cristina Bormio-Nunes¹, Clara Johanna Pacheco², Vagner de Oliveira Machado¹, Olivier Hubert³.

¹*Escola de Engenharia de Lorena, Depto de Engenharia de Materiais, Universidade de São Paulo, 12602-1810, Lorena – SP Brazil.*

²*Universidade Federal do Rio de Janeiro, LNDC/COPPE Laboratorio De Ensaio Não Destrutivos E De Corrosão (LNDC). UFRJ, 22453900 - Rio de Janeiro, RJ – Brasil*

³*École Normale Supérieure de Cachan, Laboratoire de Mécanique et Technologie, Cachan, France*

Abstract

Texture analysis of the Fe-Al-B alloy obtained by directional solidification point out to an average direction of solidification $\langle 310 \rangle$, close to $\langle 100 \rangle$. The magnetomechanical behaviour is characterized by the sensing and actuation sensitivities $d_{33} = dB/d\sigma|_H$ and $d_{33}^* = d\lambda/dH|_\sigma$, respectively. The Fe₂B phase does not act as pinning centres against domain wall movement, proved by the achieved $d_{33} \cong d_{33}^*$ reversible thermodynamic condition. This phase neither degrade the saturation magnetization of the alloy, because it has a high saturation magnetization of 1.5 T. Relatively high sensitivities of 13 kA/m/MPa were obtained for very low fields, ~ 4 kA/m, the same magnitude of that obtained in rare earth based materials, but for much lower fields. The good formability and machining properties of the Fe-Al-B alloy are also a benefit compared to rare earth based materials.

Keywords: Fe-Al-B alloy, piezomagnetic, directional solidification, magnetostriction.

1. INTRODUCTION

In the present work, we evaluate the potential improvement of the magnetostrictive behaviour obtained by directional solidification of a Fe-Al-B alloy to be employed as part of sensors and actuators. Many devices use magnetostrictive alloys and there is always a demand for more robust, easy processing and cheaper materials. A common example of application is a magnetostrictive delay line (MDL) that uses a thin magnetostrictive ribbon to measure force, magnetic field and displacement of a magnet [1]. In addition, there are torque sensors using magnetostrictive material, usually connected to crankshaft pivots and power supply shafts in motors [2]. In both cases, it is fundamental that the magnetostrictive material exhibit good magneto-mechanical coupling and actuating performance to have a high sensitivity. In addition, good mechanical properties are desirable to be mechanically conformed in many shapes and sizes depending on the application.

The magnetostrictive behaviour of the Fe-Al alloys was first studied in 1958 and the single crystal sample with the highest magnetostriction of 100 ppm was found for the composition of 19% of aluminium, a partially ordered alloy [3]. The ordering process has an important influence on the values of the saturation magnetostriction [3] [4]. The saturation magnetostriction depends strongly on the cooling rates applied to the alloy after annealing. These velocities control the stabilization of the quantities of disordered α -phase and ordered Fe₃Al phase existing in the sample [4].

For instance, the ordered phase Fe₃Al that has a D03 structure is more stable at temperatures lower than 600°C and atomic aluminum percentages lower than 20%, while the disordered α -phase that has A2 structure is more stable above this temperature and below 20%.

The addition of boron proved to be efficient on increasing the total magnetostriction of a $\text{Fe}_{80}\text{Al}_{20}$ polycrystalline alloy. A maximum magnetostriction was found for 3% of boron with an increase of 2.5 times if compared with a undoped sample alloy with the same composition. [5] [6].

The increase of magnetostriction of the $\text{Fe}_{72}\text{Ga}_{28}$ alloy doped with 1% of boron is very similar to the one observed in the mentioned Fe-Al boron doped alloy. The total saturation magnetostriction of $\text{Fe}_{72}\text{Ga}_{28}$ increases 2.2 times [7].

Chemical analysis using wavelength-dispersive spectroscopy (WDS) show that the boron atoms do not enter in the cubic lattice of the $(\text{Fe}_{0.8}\text{Al}_{0.2})_{97}\text{B}_3$ alloy and this finding is in agreement with the fact that the lattice parameter do not change with the boron addition [6]. In fact, computational modelling of the Fe-Al-B alloy with a B2 structure shows that the total energy of the system tends to increase when boron atoms enter in the matrix sites and interstices [8]. The B2 structure is also cubic and is a parent structure of A2 and D03. This calculation shows that the segregation of boron atoms at the grain boundaries is energetically favourable. The decrease of the energy happens particularly if boron occupies positions that have an iron atom as a first neighbour, favouring then the formation of the Fe_2B at the grain boundary. This is exactly the situation observed for the Fe-Al and Fe-Ga alloys [5] [6] [7]. However, $\text{Fe}_{72}\text{Ga}_{28}$ alloy doped with 1% of boron shows an increase of the crystal lattice of both A2 and D03 structures, indicating that this small atom may enter interstitially in the crystal structure of this material [7].

Concerning the microstructures, they are very similar for alloys $(\text{Fe}_{0.8}\text{Al}_{0.2})_{97}\text{B}_3$ and $(\text{Fe}_{0.72}\text{Ga}_{0.28})_{99}\text{B}_1$. In addition to the formation of the second phase Fe_2B , the coexistence of A2 and D03 structures is another important feature. In both systems, it is clear that boron modifies the solubility limits between these two cubic phases [5] [7]

[9], leading to a similar effect than the one caused by different cooling rates applied after annealing.

It is established that in Fe-Ga alloys, the intergranular segregation of the Fe₂B alloy increases the cohesion of the grain boundary and enhance the dislocation movement, promoting cross slip and eliminating the stress localized at the grain boundary, changing the fracture nature from intergranular for transgranular [9]. Due to the similarity of Fe-Al-B and Fe-Ga-B alloys, an improvement of mechanical properties is also expected for Fe-Al-B alloys.

The goal of the present work is to evaluate the magneto-mechanical behavior of the directly solidified (DS) alloy Fe-Al-B. The directional solidification is used in order to try to enhance the magnetostriction, by the formation of a favourable texture, close to <100> in the direction of solidification.

The magneto-mechanical properties are obtained from the measurements of the magnetic induction B vs mechanical applied stress σ , for several fixed values of magnetic field H. Additionally, the curves of longitudinal magnetostriction λ as a function of the magnetic field H are measured for several fixed values of mechanical stresses σ . The parameter $d_{33} = dB/d\sigma|_H$ defines the sensitivity of the material for sensing applications and $d_{33}^* = d\lambda/dH|_\sigma$ is the sensitivity of the material for actuating applications. They should lead to the same value for reversible thermodynamic conditions [10]. These coefficients are also known as piezomagnetic coefficients.

2. EXPERIMENTAL SETUP

The sample was melt using iron, aluminium and boron with high purity (< 99.9%) in an arc furnace in argon atmosphere to get an ingot of 40 g. To achieve a good homogenization, the sample was melted four times and heat treated at 1100°C for 24 hours.

After the annealing, the ingot was subjected to a hot swaging at 1100°C until reach a diameter of 6.35 mm, to fit in the alumina tube of the directional solidification system.

The swaged ingot was directionally solidified (DS) using a vertical Bridgman technique and a solidification speed of 150 mm/h.

Fig. 1 shows a home built magneto-mechanical device used to measure the magnetic induction and magnetostriction under application of magnetic field and compressive stress [11] [12]. This device has a magnetic core to close the magnetic circuit with the DS sample, shown as (a) and (e) in Fig. 1. The excitation coils are fed by a Tektronix (PWS4602 model) current source. The ends of the sample were threaded with holders of steel 4340, showed as (f) in Fig. 1, to help the alignment of the device during the compressive stress, applied by a test machine EMIC, model DL3000. The magnetic induction was measured by a pick-up coil of 75 turns, wound in the sample central region, indicated as (c) in Fig.1 and using a Lakeshore fluxmeter, model 480. The magnetostriction is measured by a Wheatstone Bridge from National Instruments (model NI9237) and Excel Sensors strain gauges with a gauge factor of 2.17, (d) in Fig. 1. Finally, a program especially designed for this application and using LabVIEW 2012, version 12.0, controls the instruments and the data acquisition.

After the magnetic characterization, the microstructure and the X-ray diffraction pattern of the sample were analysed in a transverse disk cut from exact place where the strain gauge was glued. The disks were properly prepared by standard metallographic preparation and the microstructure was analysed by a scanning electron microscopy (SEM) in a HITACHI (TM 3000 model), in the backscattered electrons mode.

X-ray diffraction experiments were performed in a Shimadzu diffractometer (XRD-6000 model) using molybdenum radiation on the same samples prepared for microscopy analyses.

The measurement of the texture of the transverse and longitudinal sections of the DS rod in the region of the magnetic measurements was performed by means of electron backscattering diffraction (EBSD). A Hitachi S-3400N scanning electron microscope was used (EDAX AMETEK).

Boron atomic concentration was determined by atomic absorption technique in an Analyst 800 from Perkin Elmer.

3. RESULTS AND DISCUSSION

Microstructural Characterization

Fig. 2 shows the X-ray diffraction pattern (XRD) of the direct solidified Fe-Al-B alloy (after annealing) and the calculated powder diffraction patterns of the phases α (A2), Fe₃Al (D03) and Fe₂B. The result shows clearly that the alloy microstructure is composed by at least two phases: α /Fe₃Al (A2/D03) and Fe₂B.

According to the diffraction prototypes of the A2 and D03 Fe-Al phases structures, the highest peaks should appear for angles close to 20° for the planes

(110)/(220) for A2 and D03 structures respectively [5]. However, the XRD measurements made on the transversal section of the DS alloy show a strong increase of the height of the peak related to the reflection of the plane (310)/(610) of A2/D03 at $2\theta \cong 45.5^\circ$. The same behaviour is also observed for peaks of (200)/(400) of A2/D03 at $2\theta \cong 28.3^\circ$. Both peaks are even higher than the peak (110)/(220). Therefore, the directional solidification produced a preferential orientation near the easy magnetization axis [100]. The peak observed at 25° can be only attributed to the plane reflection (310) of the phase Fe_2B as points the arrow in Fig. 2. Curiously, this peak is not the most intense in the Fe_2B calculated pattern, indicating that also this phase may have developed some texturing. A qualitative image analyses using the freeware program ImageJ resulted in a volumetric fraction of this phase of 6 – 7 %.

Fig. 3 depicts the micrographs of the microstructure of the DS Fe-Al-B alloy. The images show the presence of two regions with different grey tones, the light grey region corresponds to the Fe-Al matrix and the dark grey to Fe_2B spheroidal particles, just like in others works [5] [6]. The matrix composition obtained by EDX (electron dispersive X-ray) analyses resulted in concentration in atomic percentage of 79% of iron and consequently 21% of aluminium. Boron atomic concentration was determined to be 0.8%.

According to the results of XRD results and the micrographs it is not possible to resolve between A2 and D03 phase's structures. In the scanning electron microscopy the differences between the atomic weights of the cubic phases are small, therefore no difference on grey tones can be observed. Moreover, XRD peaks of the cubic phases are coincident.

EBSA analysis resulted that there are two populations of grains exhibiting two different $\langle uvw \rangle$ crystallographic direction along the direction of solidification: the first

population oriented along $\langle 931 \rangle$ and represents about 83% of the volume; the second population is oriented along $\langle 911 \rangle$ and represents about 17% of the volume. The angles made by these directions with respect to the crystallographic cubic axes ([100], [010] and [001]) are $19^\circ \pm 1^\circ$, $71^\circ \pm 1^\circ$, $84^\circ \pm 0.5^\circ$ for the first population and $12^\circ \pm 1^\circ$, $81^\circ \pm 1^\circ$, $82^\circ \pm 0.5^\circ$ for the second population. The direction of solidification is consequently corresponding to a $\langle 310 \rangle$ direction and the average angles are 17° , 73° , 84° . Indeed, these results are in accordance with the X-ray diffraction measurements.

Magnetomechanical Characterization

Fig. 4 shows the magnetic induction versus applied magnetic field for the DS Fe-Al-B alloy, after annealing, for fixed values of compressive stresses, which modulus are $\sigma = 0, 16, 48, 80, 112$ and 144 MPa.

The compressive stress introduces an extrinsic anisotropy in the material, hindering the rotation of the magnetic moments in the magnetic field direction. The consequence of this is the decrease of the slope of the B vs H curves, showed in Fig. 4, i.e. the magnetic permeability reduces as the compressive stress increases and the curves for higher σ values saturate at higher fields. Fig. 5 shows the calculated curves of the relative permeability obtained from the data of B vs H of Fig. 4. Therefore, the material needs a higher magnetic field to achieve the magnetic saturation when the compressive stress increases. The same behaviour is observed for GALFENOL and TERFENOL [13] [14] [15].

The relative permeability μ_r presents a single maximum for $|\sigma| = 0$ and 16 MPa of 420 and 235, respectively at very low fields of ~ 1 kA/m. In the interval of $16 < |\sigma| \leq 144$ MPa the μ_r curves present two maxima with values $\mu_r < 135$ and $H_{\max} \geq 5$ kA/m.

For $|\sigma| \leq 16$ MPa, the stress is not sufficiently strong to completely align $\langle 100 \rangle$ oriented domains perpendicular to the axis of the rod, in the basal plane. This regime is fully directed by the magnetocrystalline anisotropy and depends also the saturation magnetization of the material. However for $|\sigma| > 16$ MPa, the external applied stress is high enough to pin $\langle 100 \rangle$ oriented domains in the basal plane and as the field is increased the susceptibility increases steadily from zero to a maximum value at a determined field that is the field necessary to overcome the stress anisotropy. In this region the domain rotation is therefore stress dependent. In Fe-Ga alloy with 18.6% of Ga, the same behavior is observed and is associated to relatively high values of anisotropy constant (17.5 kJ/m^3) of this Fe-Ga alloy [13]. In that case the double peak appears already for $|\sigma| > 7$ MPa. The DS Fe-Al-B alloy matrix, has 21% of Al in atomic and the anisotropy constant found in the literature are $K_1 = 14.0 \text{ kJ/m}^3$ [3]. As the Fe_2B phase has a high initial susceptibility, the composite $\alpha\text{Fe-Al} + \text{Fe}_2\text{B}$ has a susceptibility that is higher than the susceptibility of the pure α -phase at low fields [16]. This improvement on the initial susceptibility can be the reason for a higher stress achieved in the single peak region of the Fe-Al-B alloy (16 MPa) compared to Fe-Ga alloy (7MPa) at low fields. Therefore the Fe_2B phase softens the Fe-Al alloy.

Fig. 6 shows the magnetostriction curves of the DS and post annealed Fe-Al-B alloy as a function of the applied magnetic field for several values of compressive stress of $0 \leq |\sigma| \leq 144$ MPa.

The directional solidification improved the longitudinal magnetostriction for $\sigma = 0$ increasing from 50 ppm in the polycrystalline Fe-Al-B alloy [5] to 69 ppm to the DS alloy¹. The field at which the magnetostriction saturates increases as the compression stress increases and the fully saturated state was not reached. However, the application of compression did not increase the saturation magnetostriction as happens in Fe-Ga

alloys [13]. This may be due to the fact that the domain distribution is already saturated so that the saturation of magnetostriction due to compression is already reached.

To determine the actuation sensitivity coefficient $d_{33} = d\lambda/dH|_{\sigma}$, the derivatives of the curves of magnetostriction vs applied field of Fig. 6 were calculated and the resulting curves are displayed in Fig. 7.

According to Fig. 7, the actuation sensitivity coefficient d_{33} is antisymmetric respect to the axis $H = 0$ and presents maxima values for fields $\pm H_{\max}$, as indicated particularly for $|\sigma| = 80$ MPa. The value of maximum d_{33} drops and H_{\max} grows as the compressive stress increases. Therefore, the material will need a higher magnetic field to achieve the best actuation coefficient. Actuation sensitivity greater than 5 nm/A occurs for $H < 7.5$ kA/m and $|\sigma| \leq 80$ MPa.

Fig. 8 illustrates the piezomagnetic behaviour of the DS Fe-Al-B alloy, which is the magnetic induction B response to a continuously varying compressive stress σ at fixed values of the magnetic field H .

The greater the variation of B with respect to σ , the greater is the sensing sensitivity of the material and this is in fact determined by the so called piezomagnetic coefficient $d_{33}^* = dB/d\sigma|_H$. The curves of d_{33}^* vs σ at fixed H values are displayed in Fig. 9.

From Fig. 9 the highest sensitivity is almost 16 T/GPa (13 kA/m/MPa) for a field of 3.9 kA/m. This is about the same magnitude of Terfenol, but for a field 5 times lower [15] [17]. The sensitivity for an interval of compressive stress $0 \leq |\sigma| \leq 80$ MPa, the sensitivity is $d_{33}^* \geq 8$ T/GPa (6.4 kA/m/MPa).

The reversible thermodynamic condition $d_{33} \cong d_{33}^*$ is reached for the DS Fe-Al-B alloy [10]. This means that the domain wall moves against anisotropy without any

pinning effect. The presence of the spheroid Fe₂B phase uniformly spread throughout the cubic phases matrix do not caused an increasing of energy dissipation.

4. CONCLUSION

The characterization of magnetomechanical behaviour of a directional solidified Fe-Al-B sample resulted that the material has relatively high sensitivity 13 kA/m/MPa, of the same order of that obtained for rare earth based materials, but for much lower fields ~ 4 kA/m. The compression window is up to 80 MPa while in rare earth based materials the maximum is 25 MPa.

The actuation and sensing sensitivities are such that $d_{33} \cong d_{33}^*$. This condition holds considering only the domain wall movement against anisotropy, because anisotropy is not negligible.

Normally, for good magnetomechanical performance low values of anisotropy constant and high values of magnetostriction are search. However, it depends also on the saturation magnetization. If for example the aluminium quantities in the alloy are increased magnetocrystalline decreases, but a simultaneous decrease of the saturation magnetization occurs.

The presence of the Fe₂B phase does not degrade the saturation magnetization of the alloy, because it has a high saturation magnetization of 1.5 T. Moreover, Fe₂B phase brings a benefit to the magnetomechanical performance because it improves the susceptibility of the alloy at low fields [13].

Nevertheless, the more crucial parameter in the magnetomechanical performance is the texture. Recently, a sensitivity of 3 kA.m⁻¹/MPa was obtained for a polycrystalline Fe-Al-B alloy [13] with comparable composition of the actual DS alloy. Therefore, an

increase of 4.3 times was achieved for the DS Fe-Al-B alloy with average orientation in the direction [310], close to [100].

5. ACKNOWLEDGMENTS

We gratefully thank FAPESP for the support under grant # 2011/21258-0. M. B.S. Dias acknowledges CAPES for the fellowship.

6. REFERENCES

- [1] E. Hristoforou
New magnetostrictive delay line arrangements for sensor applications.
Sensors and Actuators A - Physical, 81 (1-3) (2000), pp. 142-146.
- [2] Howard TS, Arthur EC, Marilyn, WF, Lawrence TK, Antonio H, Bruce B, inventors; The United States of America as represented by the Secretary of the Navy, assignee.
Magnetostrictive torque sensor.
US patent 5.201.964. 1993 Apr 13
- [3] R. C. Hall
Single Crystal Anisotropy and Magnetostriction Constants of Several Ferromagnetic Materials Including Alloys of NiFe, SiFe, AlFe, CoNi, and CoFe.
Journal of Applied Physics, 30 (1959) pp. 816-.
- [4] N. Mehmood, R. S. Turtelli, R. Grossinger, M. Kriegisch
Magnetostriction of polycrystalline Fe_{100-x}Al_x (x=15, 19, 25).
Journal of Magnetism and Magnetic Materials, 322 (210), pp. 1609-1612.
- [5] C. Bormio-Nunes, C. T. Santos, M. B. S. Dias, M. Doerr, S. Granovsky, M. Loewenhaupt
Magnetostriction of the polycrystalline Fe₈₀Al₂₀ alloy doped with boron.
Journal of Alloys and Compounds, 539 (2012), pp. 226-232.
- [6] C. Bormio-Nunes, M. B. S. Dias, L. Ghivelder
High magnetostriction of the polycrystalline alloy (Fe_{0.8}Al_{0.2}).
Journal of Alloys and Compounds, 574 (2013), pp. 467-471.

- [7] C. Bormio-Nunes, C. T. Santos, I. F. Leandro, R. S. Turtelli, R. Grössinger, M. Atif
Improved magnetostriction of Fe₇₂Ga₂₈ boron doped alloys.
 Journal of Applied Physics, 109 (2011), pp. 07A934.
- [8] J. M. Raulot, A. Fraczkiewicz, T. Cordonnier, H. Aourag, T. Grosdidier
Atomistic study of the effect of B addition in the FeAl compound.
 Journal of Materials Science, 43 (2008), pp. 3867-3872.
- [9] X. Gao, J. Li, J. Zhu, J. Li, M. Zhang
Effect of B and Cr on Mechanical Properties.
 Materials Transactions, 50 (2009), pp. 1959-1963.
- [10] D. C. Jiles, C. C. Lo
The role of new materials in the development.
 Sensors and Actuators A, 106 (2003), pp. 3-7.
- [11] M. B. S. Dias.
Construção de um transdutor quase-estático de tensão mecânica em propriedades magnéticas, aplicado á liga (Fe_{0.8}Al_{0.2})₉₈B₂ [dissertation].
 Lorena (SP): Escola de Engenharia de Lorena; 2014.
- [12] L. Weng, T. Walker, Z. Deng, M. J. Dapino, B. Wang
Major and minor stress-magnetization loops in textured polycrystalline.
 Journal of Applied Physics, 113 (2013), pp. 024508.
- [13] J. Atulasimha, A. B. Flatau, J. R. Cullen
Analysis of the effect of gallium content on the magnetomechanical behavior of single-crystal FeGa alloys using an energy-based model.
 Smart Materials and Structure. 17 (2008), pp. 8.
- [14] A. Mahadevan, P. G. Evans, M. J. Dapino
Dependence of magnetic susceptibility on stress in textured polycrystalline Fe_{81.6}Ga_{18.4} and Fe_{79.1}Ga_{20.9} Galfenol alloys.
 Applied Physics Letters, 96 (2010), pp. 012502.
- [15] X. Gao, Y. Pei, D. Fang
Magnetomechanical behaviors of giant magnetostrictive materials.
 Acta Mechanica Solida Sinica, 21 (2008), pp. 15-18.
- [16] C. Bormio-Nunes, O. Hubert
Piezomagnetic behavior of Fe-Al-B alloys.
 Journal of alloys and Compounds, submitted, April 2015.
- [17] X. Bai, C. Jiang
Dynamic parameters of Tb-Dy-Fe giant magnetostrictive alloy
 Journal of Rare Earths, 28 (2010), pp. 104-108

Footnotes

¹ Calculations from Olivier Hubert (private communication) similar to what is done in [16] produced a theoretical value of 30 ppm for isotropic Fe-Al-B with 20% of aluminum and 6% in volume of Fe₂B. The amplitude reported in [5] is due to a strong texture of the polycrystalline sample.

Figure Caption

Fig. 1 – Picture of the magnetomechanical measurement device showing: (a) the magnetic core, (b) the excitation coils (c) the pick-up coil, (d), the strain gauge, (e) the DS sample and (f) the holders.

Fig. 2 – XRD pattern for DS Fe-Al-B alloy, for 2θ in the range of 19° to 48° . The calculated powder patterns of the cubic phase's structures A2 and D03 and the Fe₂B phase are shown for comparison.

Fig. 3 - Micrographs of the annealed DS Fe-Al-B alloy for different magnification: (a) 100 \times and (b) 250 \times . Darkest particles are the phase Fe₂B and the matrix can be α and/or Fe₃Al phase.

Fig. 4 - Magnetic induction versus applied magnetic field for the DS and annealed Fe-Al-B alloy, for absolute compressive stresses values of $\sigma = 0, 16, 48, 80, 112$ and 144 MPa.

Fig. 5 - The relative permeability of the annealed Fe-Al-B alloy for absolute values of compressive stresses in the range $0 \leq \sigma \leq 144$ MPa.

Fig. 6 - Magnetostriction of the DS and annealed Fe-Al-B alloy for compressive stress of $|\sigma| = 0, 16, 48, 80, 112$ and 144 MPa.

Fig. 7 - Actuation sensitivity coefficient $d_{33} = d\lambda/dH|_{\sigma}$ of DS and annealed Fe-Al-B alloy for compressive stresses in the range $0 \leq |\sigma| \leq 144$ MPa.

Fig. 8 - Magnetic induction vs. compressive stress for several fixed values of magnetic fields for the DS and annealed Fe-Al-B alloy.

Fig. 9 - Sensitivity of the DS Fe-Al-B alloy for several magnetic fields.

Figure(if any)

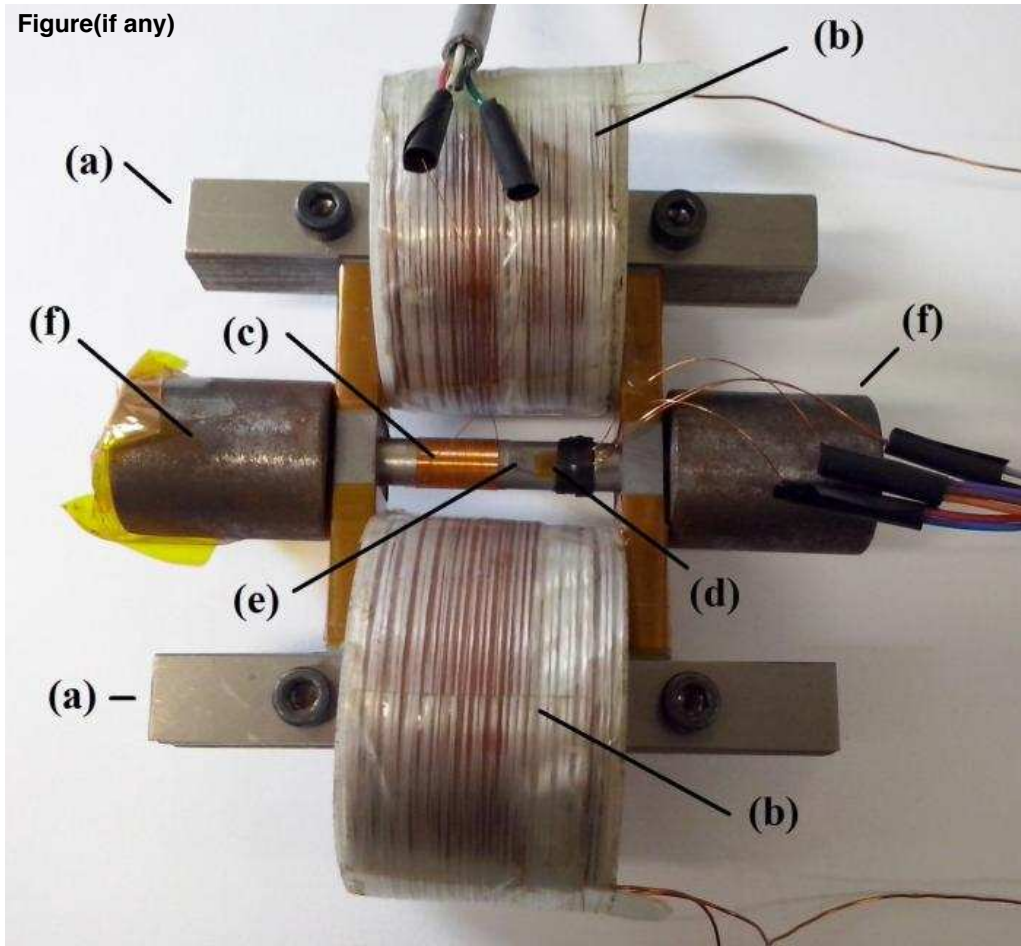


Fig. 1

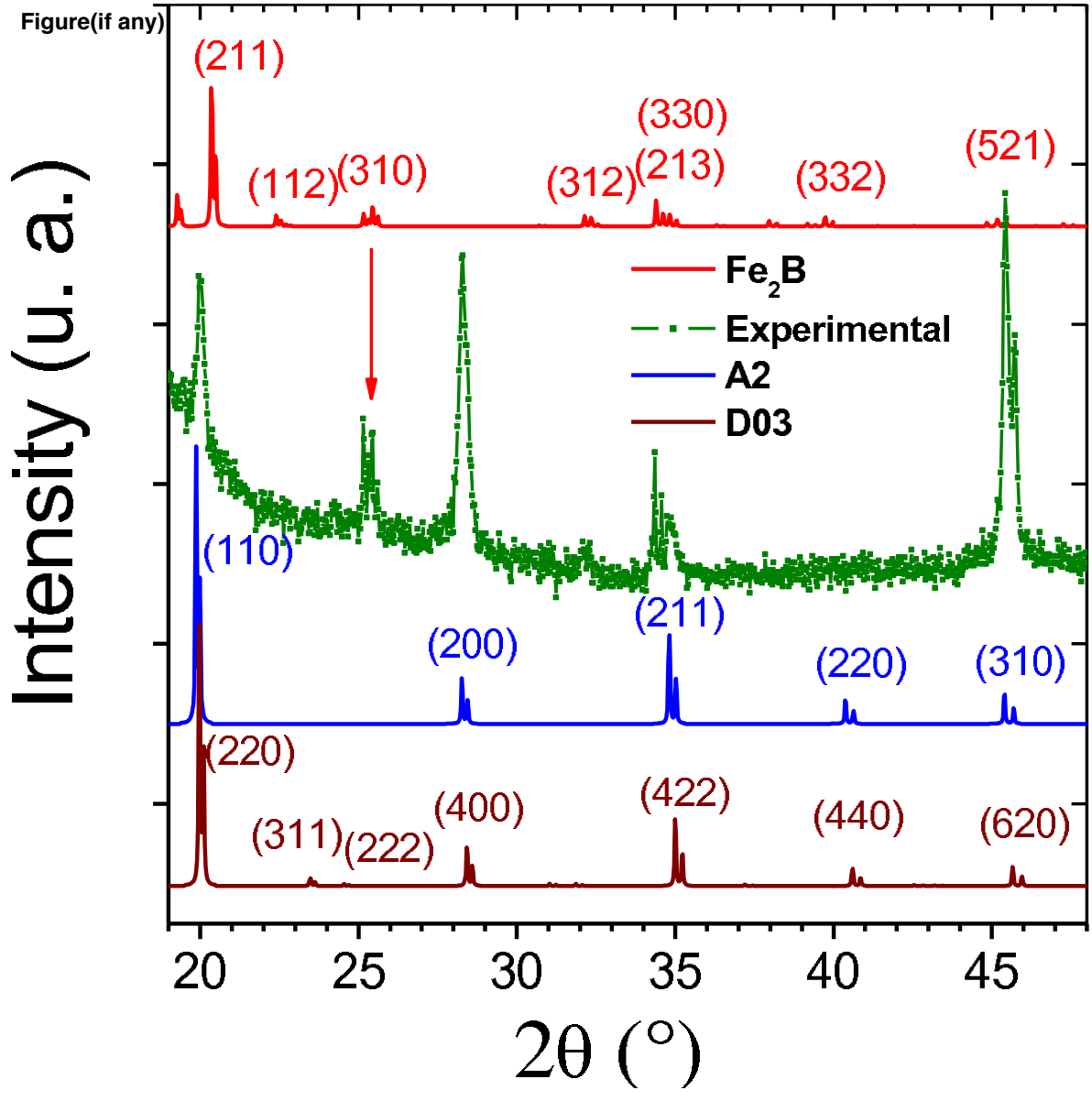


Fig. 2

Figure(if any)

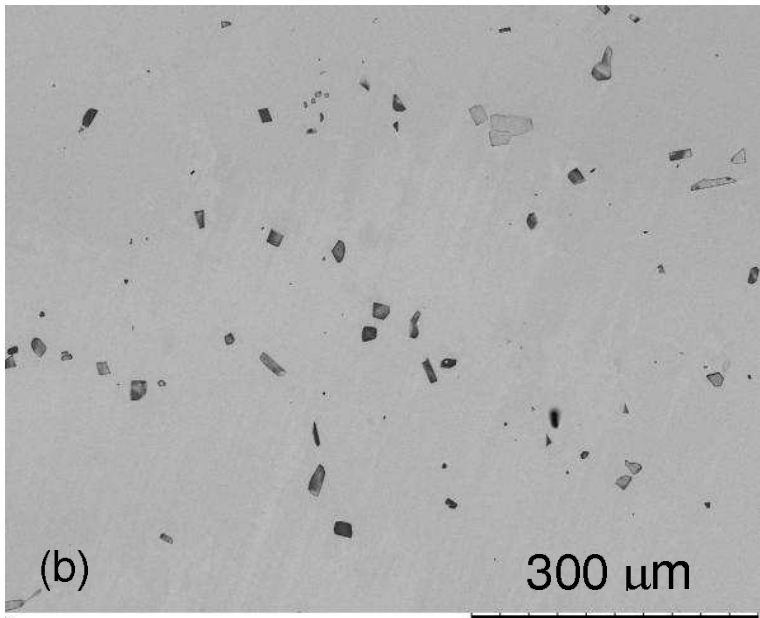
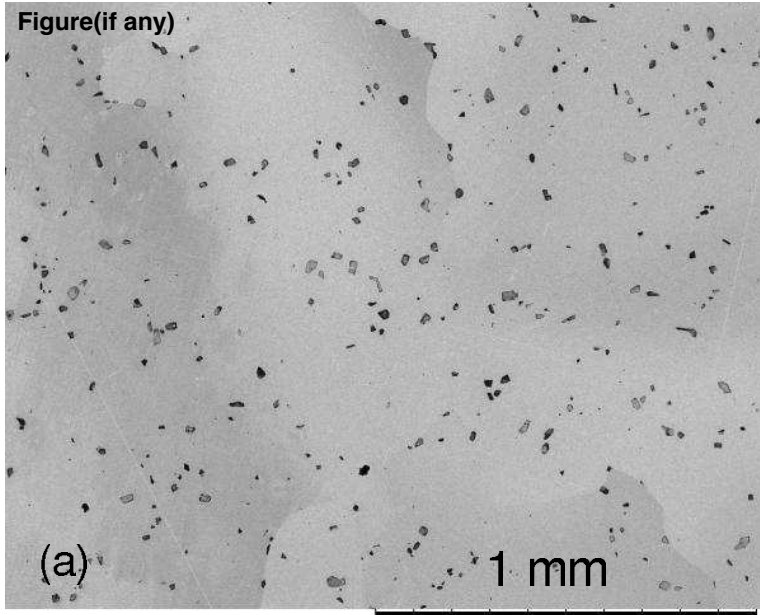


Fig. 3

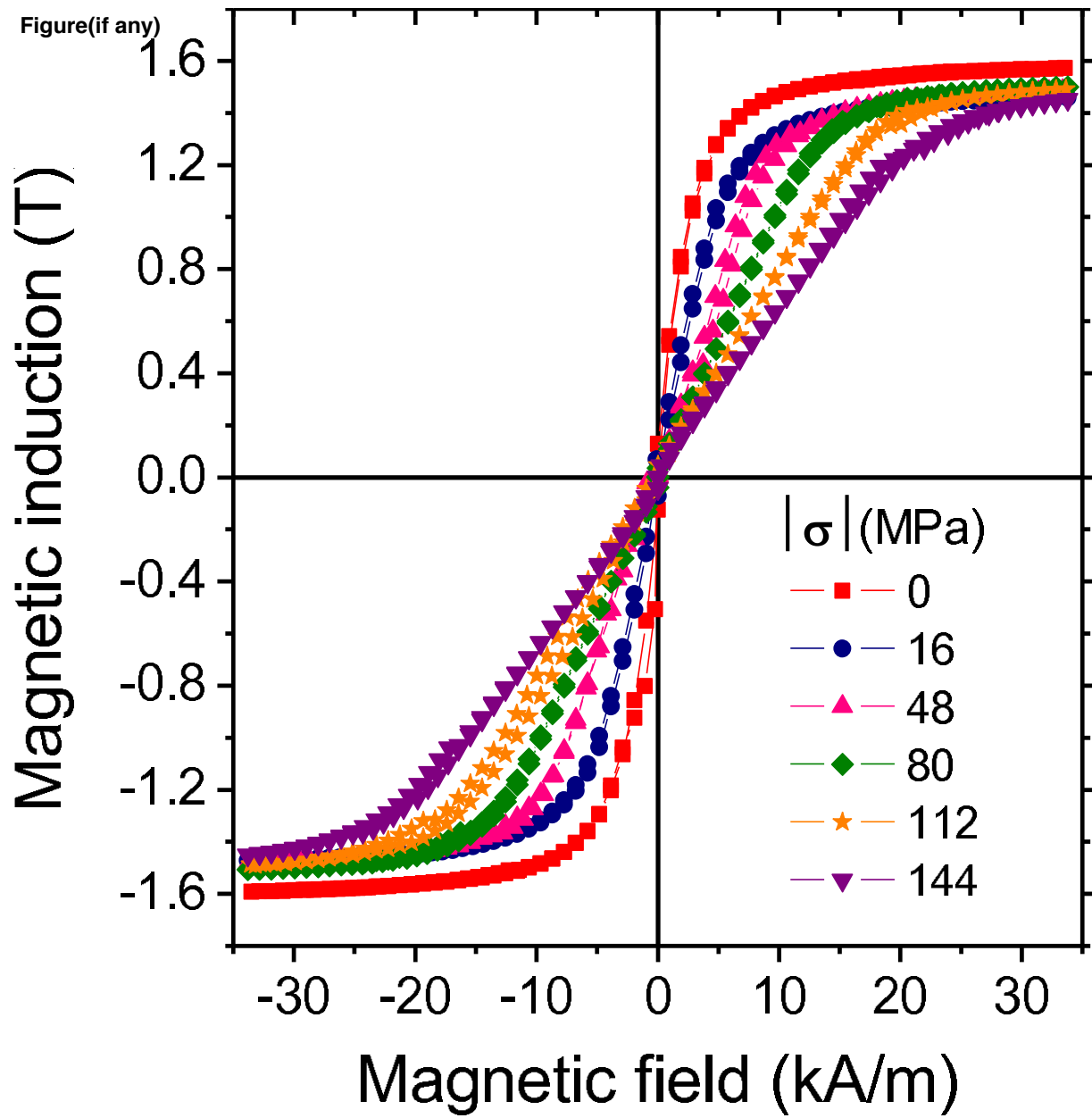


Fig. 4

Figure 5

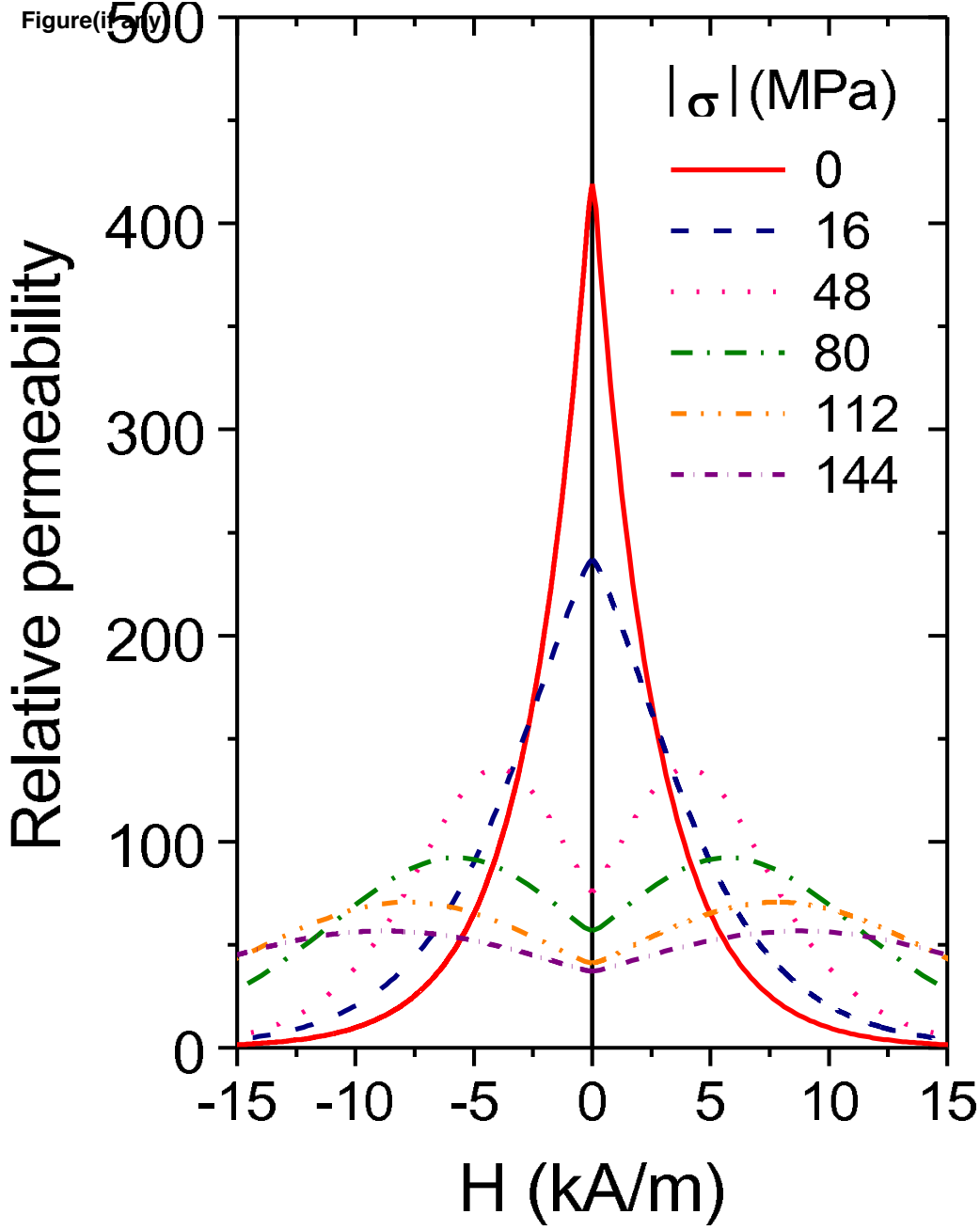


Fig. 5

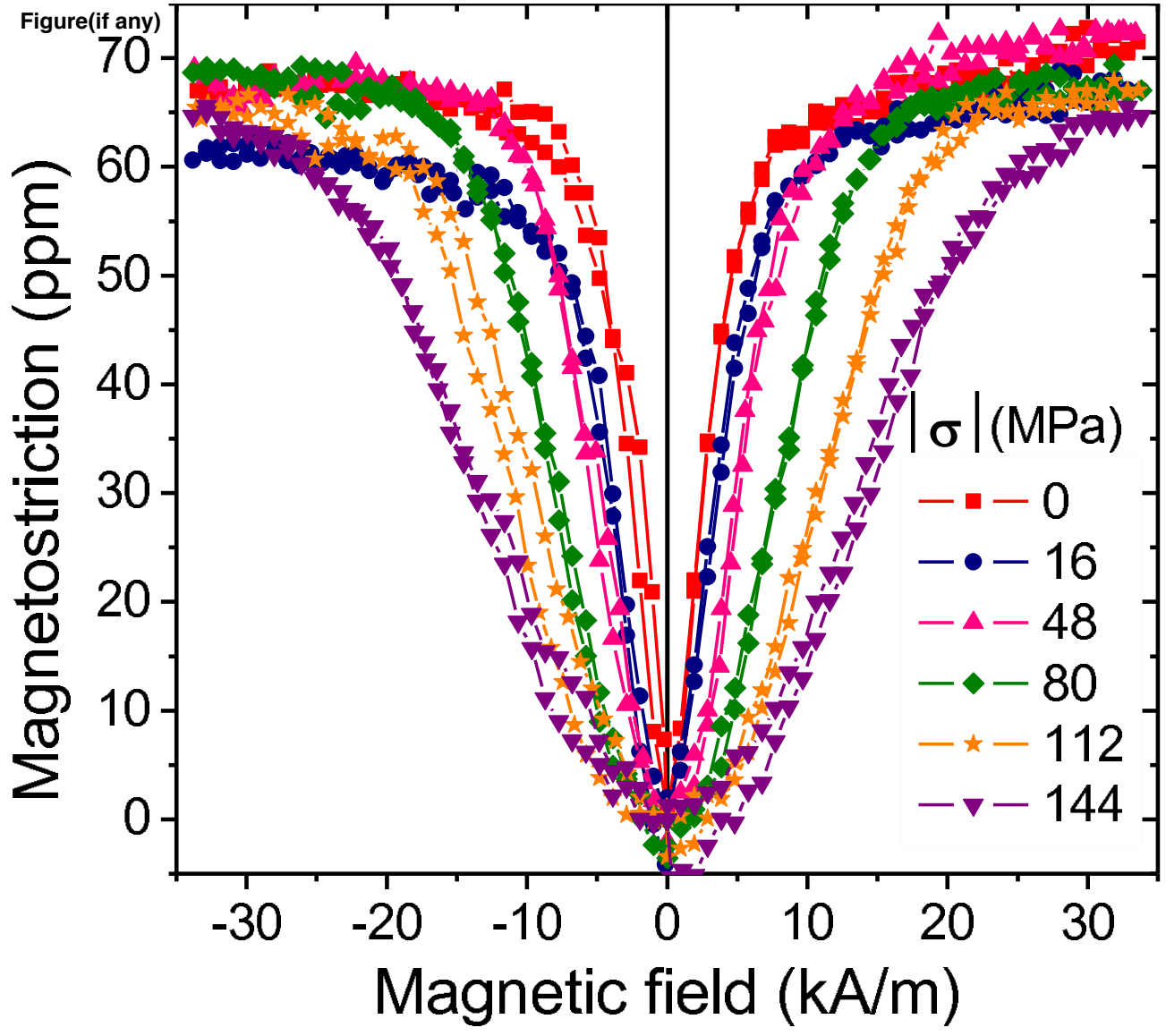


Fig. 6

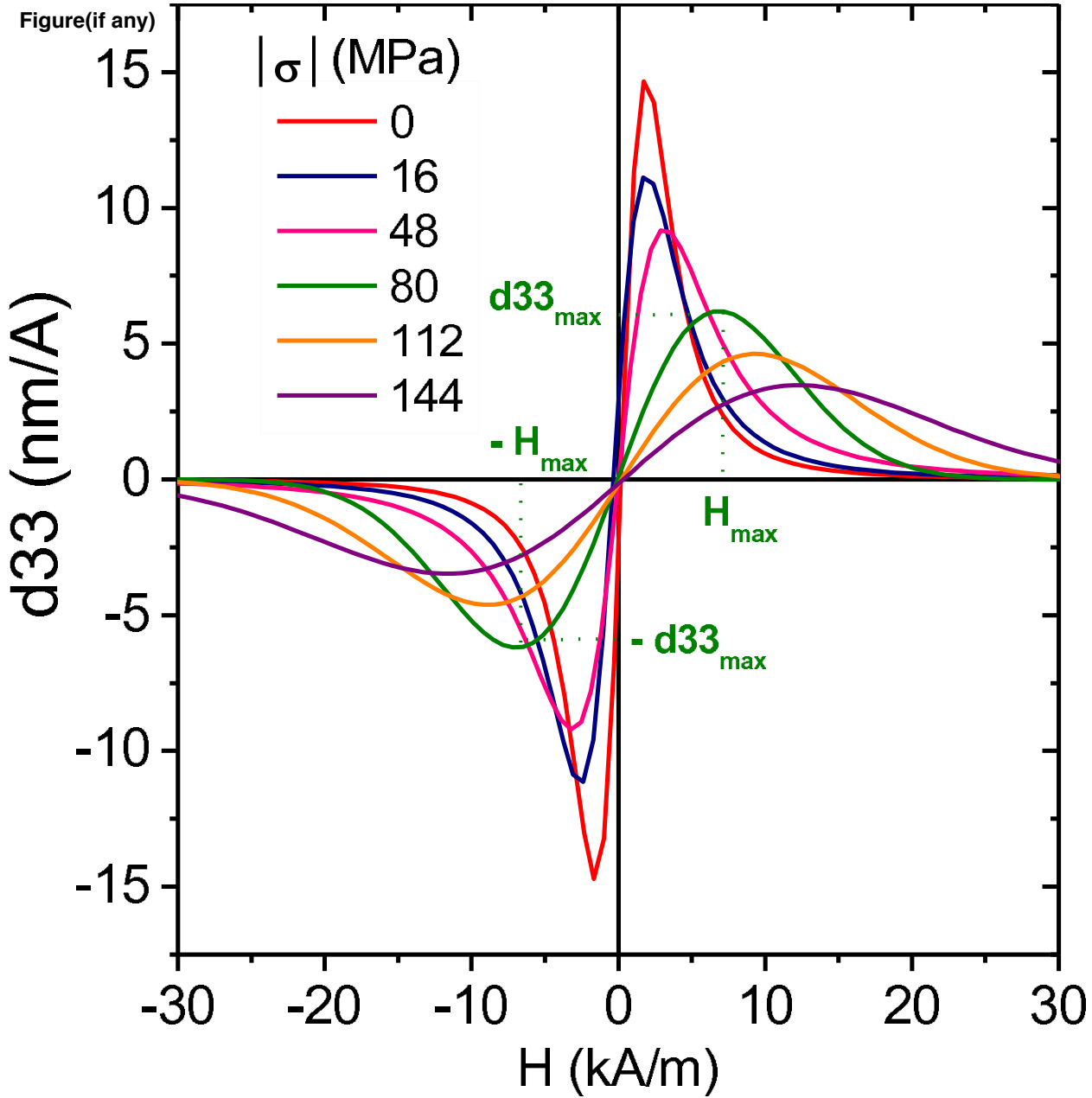


Fig. 7

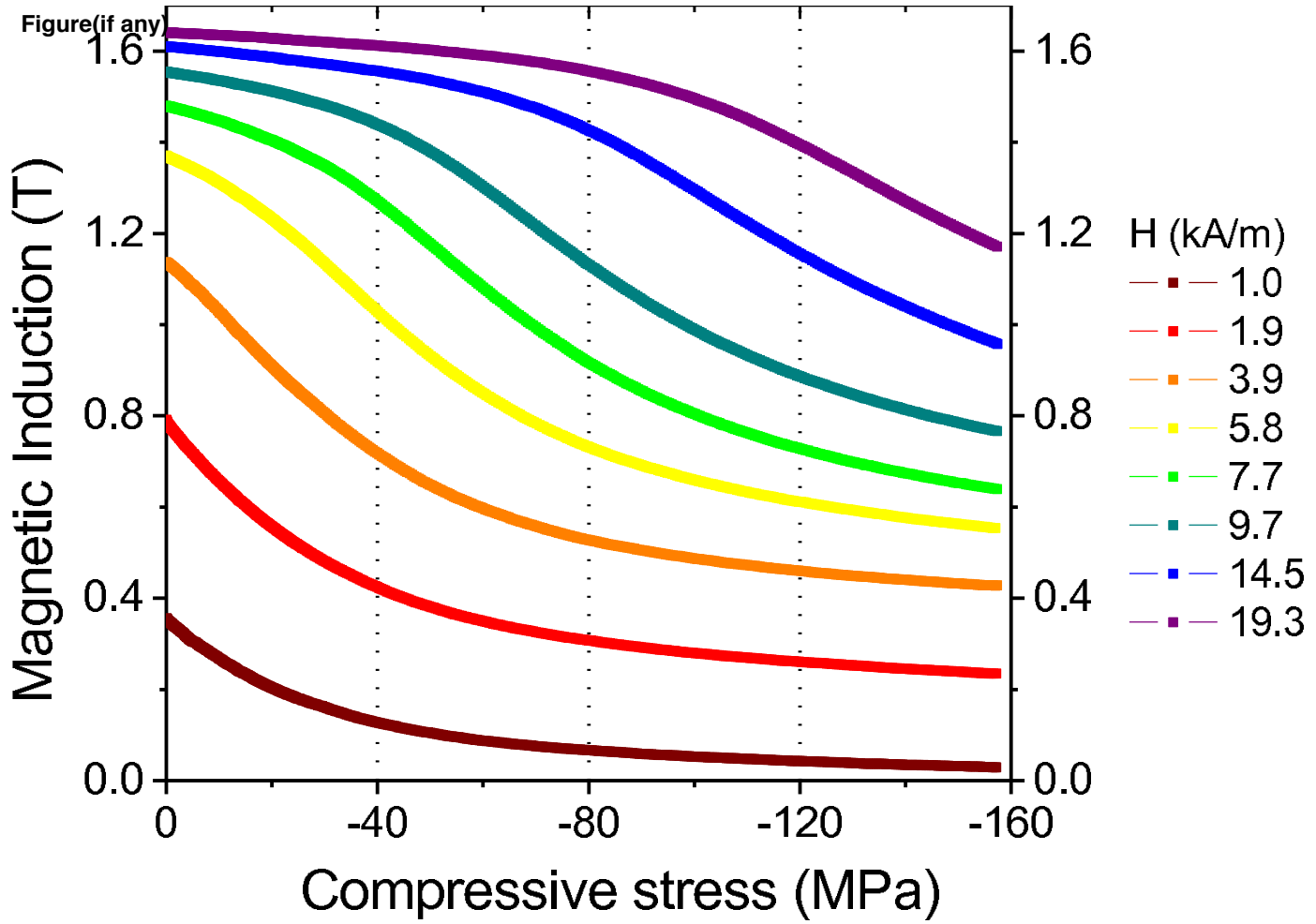


Fig. 8

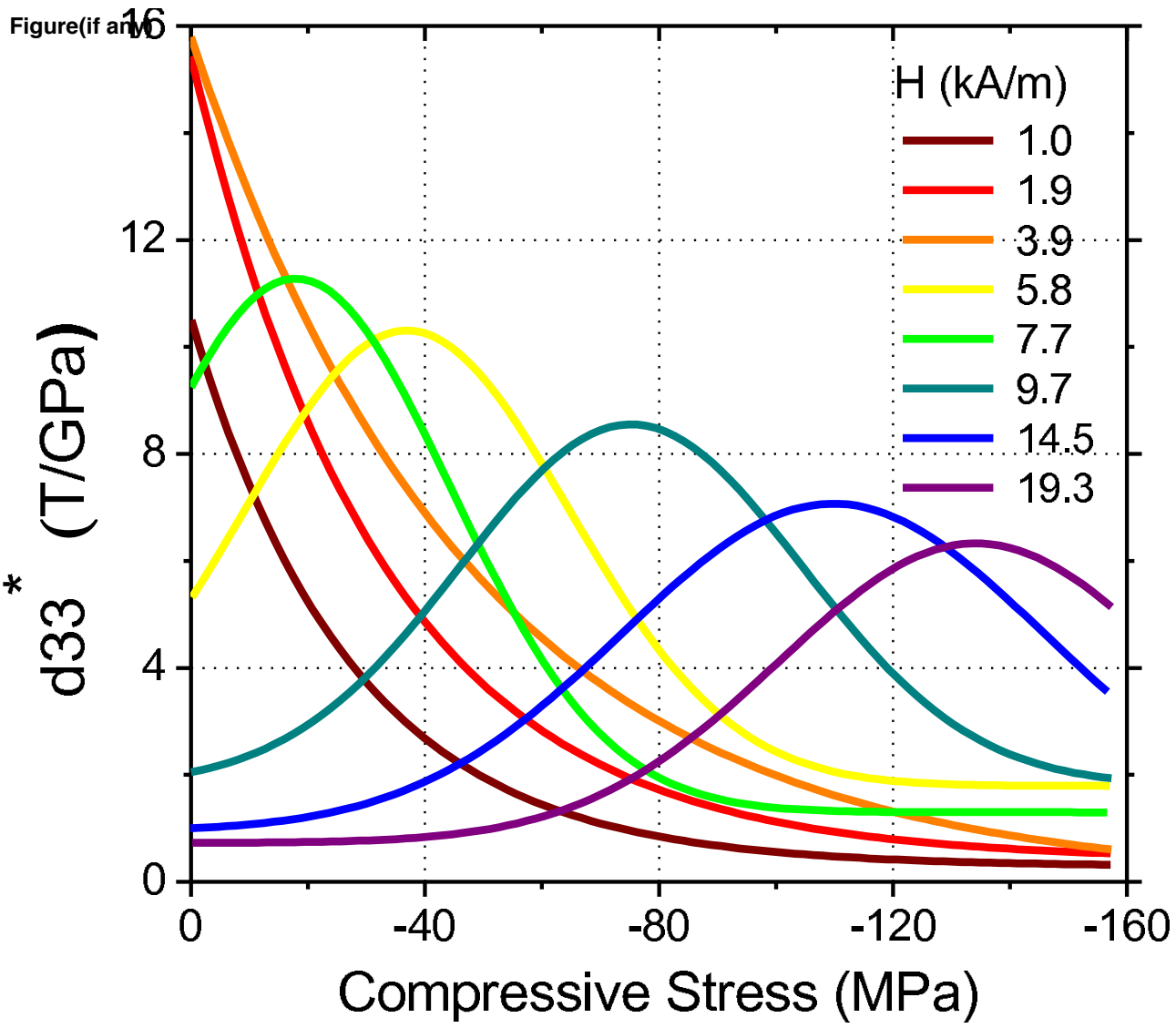


Fig. 9

Highlights

- Fe-Al-B directly solidified alloy obtained with $\langle 310 \rangle$ solidification direction.
- High magnetomechanical sensitivity of $13 \text{ kA}\cdot\text{m}^{-1}/\text{MPa}$ at 4 kA/m.
- Secondary phase Fe_2B does not cause pinning effects on domain wall movement.